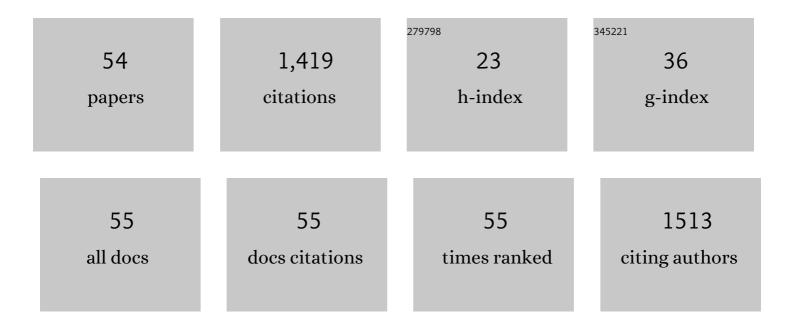
Klas Engvall

List of Publications by Year in descending order

Source: https://exaly.com/author-pdf/5423409/publications.pdf Version: 2024-02-01



KIAS ENCUAL

#	Article	IF	CITATIONS
1	Experimental and Numerical Investigation of Flow Field and Soot Particle Size Distribution of Methane-Containing Gas Mixtures in a Swirling Burner. ACS Omega, 2022, 7, 469-479.	3.5	0
2	Real-time monitoring of alkali release during CO2 gasification of different types of biochar. Fuel, 2022, 327, 125102.	6.4	11
3	Fragmentation of dolomite bed material at pressurized conditions in the presence of H2O and CO2: Implications for pressurized fluidized bed gasification. Fuel, 2021, 285, 119061.	6.4	7
4	Reaction mechanisms for H2O-enhanced dolomite calcination at high pressure. Fuel Processing Technology, 2021, 217, 106830.	7.2	12
5	Corrigendum to "Reaction mechanisms for H2O-enhanced dolomite calcination at high pressure― [Fuel Processing Technology 217 (2021) 106830]. Fuel Processing Technology, 2021, 218, 106865.	7.2	0
6	Detailed numerical simulations of low-temperature oxidation of NO by ozone. Fuel, 2021, 303, 121238.	6.4	3
7	CO ₂ Gasification Reactivity of Char from High-Ash Biomass. ACS Omega, 2021, 6, 34115-34128.	3.5	8
8	Fragmentation of dolomite bed material at elevated temperature in the presence of H2O & CO2: Implications for fluidized bed gasification. Fuel, 2020, 260, 116340.	6.4	21
9	Recent progress on parylene C polymer for biomedical applications: A review. Progress in Organic Coatings, 2020, 140, 105493.	3.9	87
10	Gas-Phase Potassium Effects and the Role of the Support on the Tar Reforming of Biomass-Derived Producer Gas Over Sulfur-Equilibrated Ni/MgAl ₂ O ₄ . Energy & Fuels, 2020, 34, 11103-11111.	5.1	6
11	Effects of Porous Structure Development and Ash on the Steam Gasification Reactivity of Biochar Residues from a Commercial Gasifier at Different Temperatures. Energies, 2020, 13, 5004.	3.1	7
12	Review and numerical investigation of the mean flow features of a round turbulent jet in counterflow. Physics of Fluids, 2020, 32, .	4.0	11
13	Investigation of the surface species during temperature dependent dehydrogenation of naphthalene on Ni(111). Journal of Chemical Physics, 2019, 150, 244704.	3.0	3
14	Experimental and modelling studies on condensation of inorganic species during cooling of product gas from pressurized biomass fluidized bed gasification. Energy, 2018, 153, 35-44.	8.8	13
15	Biomass pyrolysis gas conditioning over an iron-based catalyst for mild deoxygenation and hydrogen production. Fuel, 2018, 211, 149-158.	6.4	31
16	Modelling and Optimization of a Small Diesel Burner for Mobile Applications. Energies, 2018, 11, 2904.	3.1	6
17	Novel Model for the Release and Condensation of Inorganics for a Pressurized Fluidized-Bed Gasification Process: Effects of Gasification Temperature. ACS Omega, 2018, 3, 6321-6329.	3.5	9
18	Surface treatments of metal supports for photocatalysis applications. Applied Surface Science, 2017, 401, 283-296.	6.1	18

KLAS ENGVALL

#	Article	IF	CITATIONS
19	Selection of dolomite bed material for pressurized biomass gasification in BFB. Fuel Processing Technology, 2017, 159, 460-473.	7.2	21
20	Pyrolysis of Wood in a Rotary Kiln Pyrolyzer: Modeling and Pilot Plant Trials. Energy Procedia, 2017, 105, 908-913.	1.8	10
21	Naphthalene on Ni(111): Experimental and Theoretical Insights into Adsorption, Dehydrogenation, and Carbon Passivation. Journal of Physical Chemistry C, 2017, 121, 22199-22207.	3.1	13
22	Modeling and pilot plant runs of slow biomass pyrolysis in a rotary kiln. Applied Energy, 2017, 207, 123-133.	10.1	49
23	Equilibrium potassium coverage and its effect on a Ni tar reforming catalyst in alkali- and sulfur-laden biomass gasification gases. Applied Catalysis B: Environmental, 2016, 190, 137-146.	20.2	39
24	Modeling, Design, and Verification of a Burner for Partial Oxidation of Biomass Product Gas in an Autothermal Reformer. Industrial & Engineering Chemistry Research, 2016, 55, 9687-9697.	3.7	2
25	Biomass oxygen/steam gasification in a pressurized bubbling fluidized bed: Agglomeration behavior. Applied Energy, 2016, 172, 230-250.	10.1	71
26	A Medium-Scale 50 MWfuel Biomass Gasification Based Bio-SNG Plant: A Developed Gas Cleaning Process. Energies, 2015, 8, 5287-5302.	3.1	12
27	Model-free rate expression for thermal decomposition processes: The case of microcrystalline cellulose pyrolysis. Fuel, 2015, 143, 438-447.	6.4	34
28	Effect of gas phase alkali species on tar reforming catalyst performance: Initial characterization and method development. Fuel, 2015, 154, 95-106.	6.4	28
29	Tar Variability in the Producer Gas in a Bubbling Fluidized Bed Gasification System. Energy & Fuels, 2014, 28, 7494-7500.	5.1	6
30	Co-gasification of petroleum coke and biomass. Fuel, 2014, 117, 870-875.	6.4	115
31	Development of a PID based on-line tar measurement method – Proof of concept. Fuel, 2013, 113, 113-121.	6.4	19
32	Application of Solid-Phase Microextraction (SPME) as a Tar Sampling Method. Energy & Fuels, 2013, 27, 3853-3860.	5.1	6
33	Modelling and Simulation of Biomass Conversion Processes. , 2013, , .		1
34	Engineering of bone fixation metal implants biointerface—Application of parylene C as versatile protective coating. Materials Science and Engineering C, 2012, 32, 2431-2435.	7.3	28
35	Iron-based materials as tar depletion catalysts in biomass gasification: Dependency on oxygen potential. Fuel, 2012, 95, 71-78.	6.4	69
36	Parylene coatings on stainless steel 316L surface for medical applications — Mechanical and protective properties. Materials Science and Engineering C, 2012, 32, 31-35.	7.3	47

KLAS ENGVALL

#	Article	IF	CITATIONS
37	Silane–parylene coating for improving corrosion resistance of stainless steel 316L implant material. Corrosion Science, 2011, 53, 296-301.	6.6	111
38	Defluidisation of fluidised beds during gasification of biomass. Biomass and Bioenergy, 2011, 35, S63-S70.	5.7	26
39	Biomass gasification in an atmospheric fluidised bed: Tar reduction with experimental iron-based granules from HöganäAB, Sweden. Catalysis Today, 2011, 176, 253-257.	4.4	29
40	Development of an on-line tar measurement method based on photo ionization technique. Catalysis Today, 2011, 176, 250-252.	4.4	15
41	Upgrading of Raw Gas from Biomass and Waste Gasification: Challenges and Opportunities. Topics in Catalysis, 2011, 54, 949-959.	2.8	25
42	Metal release and formation of surface precipitate at stainless steel grade 316 and Hanks solution interface – Inflammatory response and surface finishing effects. Corrosion Science, 2009, 51, 1157-1162.	6.6	38
43	High Pressure Desorption of K+from Iron Ammonia Catalyst – Migration of the Promoter Towards Fe Active Planes. Catalysis Letters, 2004, 95, 93-97.	2.6	6
44	A Surface Ionization Instrument for On-Line Measurements of Alkali Metal Components in Combustion:  Instrument Description and Applications. Energy & Fuels, 2002, 16, 1369-1377.	5.1	46
45	Desorption Kinetics at Atmospheric Pressure:Â Alkali Metal Ion Emission from Hot Platinum Surfaces. Journal of Physical Chemistry B, 2000, 104, 4457-4462.	2.6	21
46	Cluster KN formation by Rydberg collision complex stabilization during scattering of a K beam off zirconia surfaces. Journal of Chemical Physics, 1999, 110, 1212-1220.	3.0	43
47	Long-Range Diffusion of K Promoter on an Ammonia Synthesis Catalyst Surface—lonization of Excited Potassium Species in the Sample Edge Fields. Journal of Catalysis, 1999, 181, 256-264.	6.2	34
48	In situ characterization of an iron catalyst by potassium ion desorption and electron emission measurements. Reaction Kinetics and Catalysis Letters, 1998, 63, 219-224.	0.6	7
49	Angular resolved neutral desorption of potassium promoter from surfaces of iron catalysts. Surface Science, 1995, 342, 327-340.	1.9	40
50	Emission of excited potassium species from an industrial iron catalyst for ammonia synthesis. Catalysis Letters, 1994, 26, 101-107.	2.6	35
51	Field ionisation of excited alkali atoms emitted from catalyst surfaces. Applied Surface Science, 1992, 55, 303-308.	6.1	30
52	Comparative loss of alkali promoter by desorption from two catalysts for the dehydrogenation of ethyl benzene to styrene. Applied Catalysis, 1991, 77, 235-241.	0.8	30
53	Loss of alkali promoter by desorption from promoted vanadium oxide catalysts. Catalysis Letters, 1991, 11, 41-48.	2.6	18
54	Mechanism of potassium loss by desorption from an iron oxide catalyst for the styrene process. Catalysis Letters, 1990, 6, 85-93.	2.6	40